Effects of a large-scale mean circulating flow on passive scalar statistics in a model of random advection

Emily S. C. Ching,[1] C. S. Pang,[1] and Gustavo Stolovitzky[2]
[1]*Department of Physics, The Chinese University of Hong Kong, Shatin, Hong Kong*
[2]*Center for Studies in Physics and Biology, Rockefeller University, New York, New York 10021*
(Received 24 December 1997)

We study the effects of a large-scale mean circulating flow on passive scalar statistics in turbulent advection using a two-dimensional lattice model. The incompressible advecting velocity field consists of a large-scale circulation plus fluctuations. The latter are modeled by a random Gaussian field that has a finite correlation time but is statistically independent at different lattice points. In the presence of the large-scale flow, we find that the profiles of both the mean and the rms fluctuation of the passive scalar are modified significantly, and have close resemblance to those observed experimentally in turbulent convection. The one-point probability density functions (PDFs) of the passive scalar at the two sides are affected by the large-scale flow and become more skewed. There is, however, not much change for the PDFs at other locations. Furthermore, the shape of the PDFs of the scalar increments remains the same with or without the presence of the large-scale flow, supporting the idea that large-scale effects can be filtered out by studying increments.
[S1063-651X(98)08008-8]

PACS number(s): 47.27.−i

I. INTRODUCTION

High-Rayleigh-number convection in fluid enclosed in a cell is often taken as a system for investigating fluid turbulence as the boundary conditions are well defined and the flow can be changed from laminar to turbulent in a controlled manner. Many interesting features have been uncovered [1]. A scaling state, which covers a wide range of Rayleigh number (Ra) from 10^8 to 10^{15}, was revealed [2]. This turbulent regime is characterized by power-law dependence of the heat flux and the size of local temperature fluctuations with Ra, and has various features that have attracted much attention. First, the scaling exponent of the heat flux is 2/7, which is different from 1/3, the value one might obtain from ideas of marginal stability [3], which suppose that the top and the bottom thermal boundary layers do not interact. Second, the probability distribution of temperature fluctuations at the center of the cell was found to be exponential (as opposed to the Gaussian observed at lower values of Ra). Finally, there is a persistent large-scale mean circulating flow that spans the whole experimental cell [4], and the velocity of the flow also scales with Ra. The presence of a large-scale flow naturally induces an interaction between the two thermal boundary layers. Two different theoretical models [5,6] have been proposed to derive the scaling laws. In particular, the effect of the shear produced by the mean circulating flow on the heat flux was studied explicitly in Ref. [6]. However, a complete understanding is still lacking [7–10]. More recently, it was further found that the distribution of temperature fluctuations become a superposition of two Gaussians when the large-scale flow is perturbed [11].

In thermal convection, the temperature field takes part in driving the flow and is so-called active. In this situation, the velocity and the temperature fields are coupled in a complicated manner. On the other hand, the problem of a passive temperature field, i.e., a temperature field that is advected by a *given* velocity field, is simpler. Insights or understanding of some features of thermal convection may be gained by studying a passive scalar subjected to a suitably prescribed velocity field. As a result, various studies [12–18] were motivated to understand when the statistics of a randomly advected passive scalar will be non-Gaussian.

Along the same line of thoughts, it would be interesting to study how the presence of a large-scale mean circulating flow might affect the passive scalar statistics in turbulent advection. In this paper, we report the results from a numerical study. We use a two-dimensional lattice model [17,19] in which the fluctuation of the incompressible velocity field is mimicked by a random Gaussian field that has a finite correlation time but is statistically independent at different lattice points. In earlier studies, it was found [17] that the passive scalar fluctuation becomes non-Gaussian for a certain range of parameters of the model. Moreover, this change in statistics is independent of the one-point statistics prescribed for the velocity field [19]. In the present study, we introduce a large-scale mean circulating flow into the model and find that its presence modifies the profiles of both the mean and the rms fluctuation of the passive scalar significantly. Interestingly, these profiles now show close resemblance to the corresponding profiles for the temperature field observed experimentally in turbulent convection [7]. The one-point probability density functions (PDFs) of the passive scalar at the two sides are affected by the large-scale flow and become more skewed. There is, however, not much change for the PDFs at other locations. Furthermore, the shape of the PDFs of the scalar increments remains the same with or without the presence of the large-scale flow, supporting the idea that large-scale effects can be filtered out by studying increments.

II. MODEL

We use a two-dimensional lattice model to study the advection of a passive scalar by a random incompressible ve-

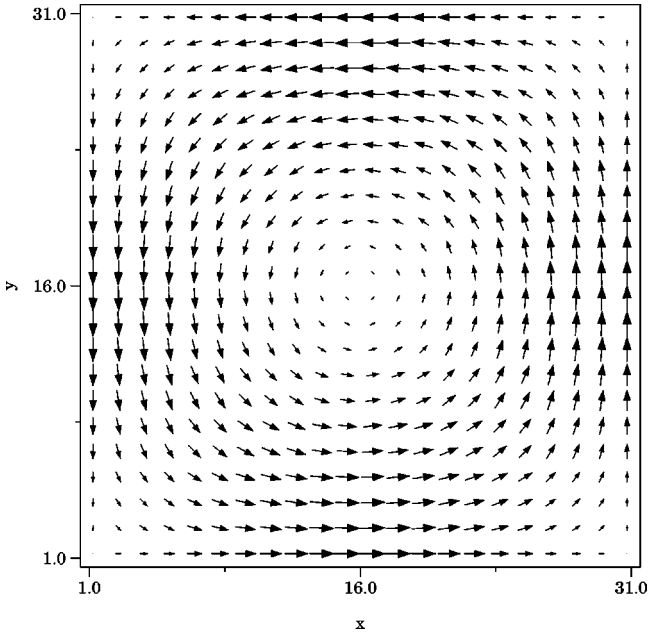

FIG. 1. The velocity field generated from the time-independent term ϕ_m in the stream function for $A=0.4$. The size of the arrow indicates the relative magnitude of the velocity.

locity field. The model was discussed in Refs. [17,19]. Here, we outline the main points and the new features introduced in the present study. We solve numerically the discrete advection-diffusion equation for the scalar $T(i,j,t)$ on a $N \times N$ square lattice of spacing ξ:

$$\frac{\partial T(i,j,t)}{\partial t} + \mathbf{u}(i,j,t)\cdot\nabla_{ij} T(i,j,t) = D\nabla_{ij}^2 T(i,j,t), \quad (1)$$

where D is an effective eddy diffusivity, and $i,j = 1,\ldots,N$. The length of the square lattice is, therefore, $L = N\xi$. The parameter D should not be identified with the molecular diffusivity since, by construction, the smallest spatial scales are not resolved.

The incompressible advecting velocity field $\mathbf{u}$ is generated from the stream function $\phi(x,y,t)$, which consists of a time-independent and a fluctuating part:

$$\phi(x,y,t) = \phi_f(x,y,t) + \phi_m(x,y). \quad (2)$$

The fluctuating part, $\phi_f(x,y,t)$, is taken to be a random Gaussian field, identically independently distributed at each lattice point, with zero mean, standard deviation ϕ_0, and correlation time τ_c [17,19]. In the present study, we introduce the time-independent term, ϕ_m:

$$\phi_m(x,y) = \frac{AL}{\pi}\sin\left(\frac{\pi x}{L}\right)\sin\left(\frac{\pi y}{L}\right), \quad (3)$$

which gives rise to a large-scale circulation as shown in Fig. 1. As seen from Fig. 1, this large-scale flow does not satisfy the no-slip condition at the boundaries. However, as we shall see, this has little effect on the passive scalar PDF at locations away from the boundaries.

The typical size of the velocity fluctuation is given by $u_0 \equiv \phi_0/\xi$. The correlation length of the velocity field is ξ even with the presence of the large-scale mean circulating flow. There are three independent dimensionless parameters in the problem, which we take as $K = u_0\tau_c/\xi$, $C = \xi^2/(D\tau_c)$, and the ratio A/u_0. The parameters K and C are respectively the ratio of the velocity correlation time to the advection time and the ratio of the eddy-diffusion time to the velocity time while the ratio A/u_0 measures the relative strength of the mean and the fluctuating velocities. It is known from previous studies [17,19] that in the case without a mean flow ($A=0$), the one-point PDF of the passive scalar at the center of the lattice varies from a Gaussian to a distribution with flatter-than-Gaussian tails as C increases when K is fixed. In the present study, we fix $K=1.0$ and $C=8.0$, values at which the one-point PDF is nearly exponential [17,19] when $A=0$, and study the possible effects of the presence of a large-scale mean circulating flow by comparing the results for $A=0$ with those for $A\neq 0$, e.g., $A/u_0=0.05$.

Equation (1) is integrated in time using the finite difference method with a small time step $\Delta t=0.005$, and $N=31$. Such a relatively small size is sufficient as we shall evaluate the statistics by averaging over time. The fluctuating part of the stream function, ϕ_f, is updated every $m=25$ time steps at each lattice site so that $\tau_c = m\Delta t = 0.125$. The boundary conditions for the scalar field are (i) a fixed difference along the j direction: $T(i,j=0,t)=0$ and $T(i,j=N+1,t)=1$; and (ii) vanishing horizontal gradient at $i=1$ and $i=N$. For the velocity field, we adopt a free boundary condition since our large-scale mean circulating flow (3) does not satisfy the no-slip boundary condition. In Fig. 2, we check the effect of this nonphysical boundary condition for $A=0$. It can be seen that the passive scalar PDFs near the top and the bottom boundaries remain exponential with a larger flatness as compared to the PDFs for the no-slip boundary condition while the PDFs at other locations are not affected.

III. RESULTS AND DISCUSSIONS

We first compare the mean scalar profile $\langle T\rangle$, averaged over time, for $A=0$ and $A/u_0=0.05$. From Fig. 3, we immediately notice that the mean scalar profile is modified significantly in the presence of a large-scale flow. For $A=0$ (squares) which corresponds to the absence of a large-scale mean flow, $\langle T\rangle$ has been found to be linear in the j direction [17,19] with little dependence on i. For $A/u_0=0.05$ (circles), the profile has a very different shape. At fixed i, $\langle T\rangle$ shows a comparatively flat region near the center of the lattice with the gradient steepened near the two boundaries $j=1$ and $j=N$. Moreover, an overall horizontal gradient is developed. Reversal of this horizontal gradient is observed when either the flow direction or the applied scalar difference is reversed. We thus attribute this horizontal gradient to the presence of the large-scale flow, which brings more ''hot'' fluid to $i=1$ and more ''cold'' fluid to $i=31$. A similar effect of the large-scale flow generating a horizontal variation in the mean temperature of the top and the bottom plates was observed by Cioni *et al.* in thermal convection [20]. The time-independent profile when the velocity field is solely the large-scale circulation with no fluctuation (with the same value of A) is evaluated and plotted as the solid line. Good agreement between the solid line and the circles can be seen.

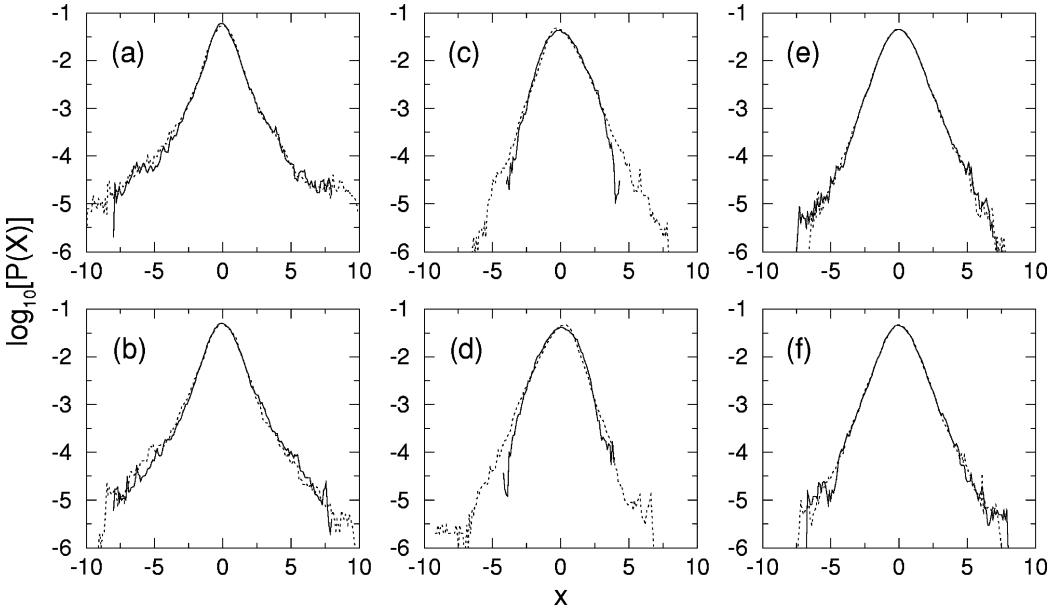

FIG. 2. Comparison of the normalized PDFs, $P(X)$ for $X=(T-\langle T\rangle)/\sigma$ and σ is the rms fluctuation, at various locations: (a) $(i=1,j=16)$, (b) $(i=31,j=16)$, (c) $(i=16,j=1)$, (d) $(i=16,j=31)$, (e) $(i=8,j=8)$, and (f) $(i=16,j=16)$, for two different sets of boundary conditions for the velocity field with $A=0$: periodic in the x direction, no slip in the y direction (solid line), and free in all boundaries (dotted line). The boundary conditions for the scalar field are the same.

It is interesting to note that the profile for $A\neq 0$ has close resemblance to the mean temperature profile observed experimentally in turbulent convection [7]. In turbulent convection, a temperature difference is applied along the vertical direction. It was observed that in the steady state, the applied temperature difference concentrates in two thin thermal boundary layers at the top and the bottom plates and the central region of the experimental cell is almost statistically isothermal. Moreover, as discussed in Sec. I, a large-scale flow is self-generated by the applied temperature difference. Once the large-scale flow is generated, the temperature field will be advected in a similar manner as in the case of a passive scalar except that the interaction between the velocity and the temperature fields is now two-way. Our results thus show that the shape of the mean temperature profile observed in thermal convection is a direct consequence of the presence of a large-scale mean circulating flow.

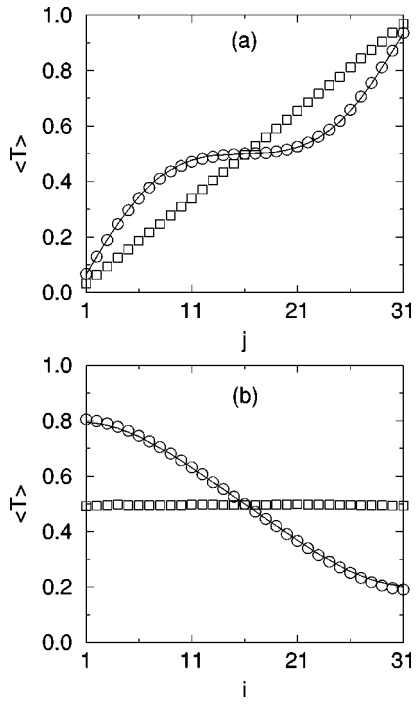

FIG. 3. Mean scalar profile (a) $\langle T(i=16,j)\rangle$ and (b) $\langle T(i,j=16)\rangle$ for the two cases $A=0$ (squares) and $A/u_0=0.05$ (circles). Shown also are the time-independent profiles for the velocity field being solely the large-scale circulating flow with no fluctuation (solid lines).

In Fig. 4, we compare the profiles for the rms scalar fluctuation σ. For $A=0$, σ is approximately constant at $i=16$ except near the boundaries. As T is fixed at the top and the

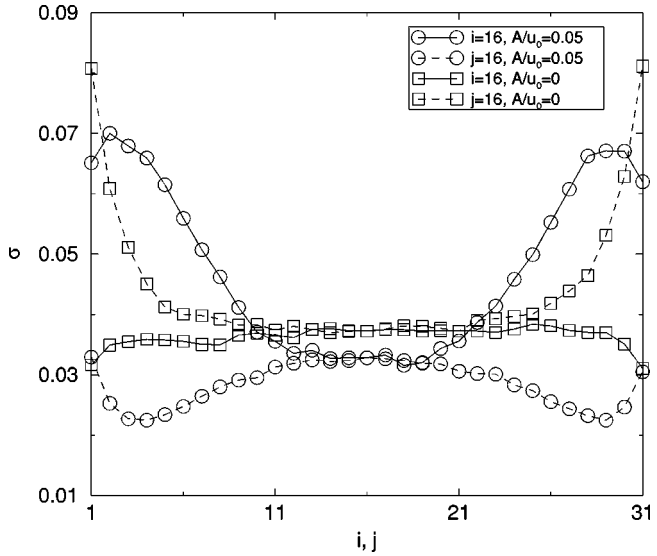

FIG. 4. Rms scalar fluctuation profile for $A=0$ (squares) and $A/u_0=0.05$ (circles).

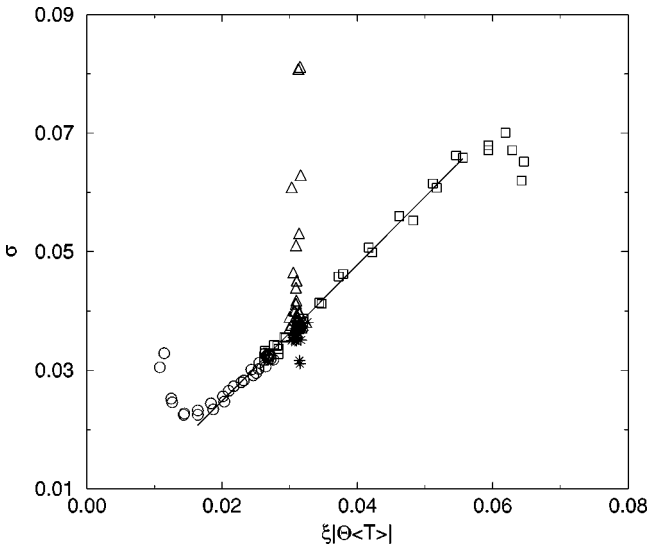

FIG. 5. A plot of $\sigma(i,j)$ vs $\xi|\nabla T|$ for $A=0$ [$i=16$ (stars), $j=16$ (triangles)] and $A/u_0=0.05$ [$i=16$ (squares), $j=16$ (circles)]. The slope of the fitted line is 1.15, of order 1, supporting the prediction of Ref. [14]. The data points that deviate from the straight line correspond to data taken near the boundaries where the PDF deviates from an exponential.

bottom boundaries, we expect σ to be smaller near $j=1$ and $j=31$ as observed. For fixed $j=16$, on the other hand, σ is larger near $i=1$ and $i=31$ as T is not specified near the side boundaries. For $A\neq 0$, σ is generally smaller, indicating that mixing is enhanced in the presence of the large-scale flow. Around the top and the bottom boundaries, $j=1$ and $j=31$, σ is, however, relatively larger in the presence of the large-scale flow because the scalar gradient is amplified there. Thus, the two profiles look very different. In the j direction, σ is maximum near the center of the lattice for $A=0$ but a minimum for $A\neq 0$ while the reverse is true along the i direction. The dependence of σ along the vertical (j) direction in the presence of a large-scale flow again resembles that observed in turbulent convecton experiments [7].

According to Ref. [14], when the Peclet number is large enough and when there is a local gradient in the mean scalar profile, the scalar PDF will be exponential with a velocity-independent rms fluctuation given by

$$\sigma_{\mathrm{PSS}}\sim \xi|\nabla\langle T\rangle|. \tag{4}$$

For $A=0$, $\nabla\langle T\rangle$ is almost the same at each lattice point, thus σ should be approximately constant by Eq. (4). For $A/u_0=0.05$, a plot of σ versus $\xi|\nabla\langle T\rangle|$ should give a straight line with a slope of the order 1. We plot σ against $\xi|\nabla\langle T\rangle|$ in Fig. 5, and the results are as expected whenever the scalar PDF is nearly exponential. The data points that show deviations are measured from locations near the boundaries where the scalar PDF is skewed and deviates from an exponential (see below). Thus, the rms scalar fluctuation profile, within the bulk of the lattice, can be understood from the mean scalar profile together with Eq. (4).

In earlier work [17,19], we have focused on the one-point scalar PDF at the center of the lattice and have studied its dependence on the parameters K and C when there is no mean flow. In the present study, we study also the PDFs at other locations. When there is no mean flow, the PDF is found to be the same at every lattice point within the bulk of the lattice. At lattice points near the top and the bottom boundaries, the PDF is noticeably skewed. It is positively skewed near the bottom and negatively skewed near the top. This asymmetry is due to the fixed difference boundary condition, which leads to more ''hot'' fluctuation near the bottom ''cold'' boundary and vice versa. The PDFs near the two sides are also skewed and with the same sign. In the presence of the large-scale flow, the shape of the PDF remains nearly exponential. A major effect is that the PDFs near the two sides become more skewed, with the PDF on the left (near $i=1$) being positively skewed while that on the right (near $i=31$) is negatively skewed (see Fig. 6). On the other hand, the PDFs at the other locations are not affected much by the large-scale flow. The asymmetry of the PDF near the two sides can be understood as a result of the anisotropy introduced by the large-scale flow, which brings more ''hot'' fluid to $i=1$ and more ''cold'' fluid to $i=31$.

In Fig. 7, we plot the skewness of the PDF as a function of the location for the two cases. The scalar field at any lattice point is coupled to the scalar field at neighboring points. Suppose there is gradient in the mean scalar profile at a certain point (i,j), then larger or smaller fluctuations will reach it from the neighboring points. Suppose there is also a gradient in the rms fluctuation profile at (i,j), then the typical sizes of fluctuation from the neighboring points will be different. Thus, there will be relatively more large or small fluctuations implying that the PDF at (i,j) is skewed. Hence, the PDF at a particular point will be skewed if there is nonvanishing local gradient in both the mean *and* the rms fluctuation profiles at that point. This observation is generally verified by comparing Fig. 7 with Fig. 3 and Fig. 4. Moreover, the sign of the skewness can be generally understood, using similar arguments, from the signs of the gradients of the mean and the rms fluctuation profiles.

It is known that [21] the PDF of a stationary fluctuation $X(t)$, with zero mean and unit standard deviation, is related to two conditional averages of its time derivatives:

$$P(x)=\frac{C_N}{\langle \dot{X}^2|X=x\rangle}\exp\left[\int_0^x \frac{\langle \ddot{X}|X=x'\rangle}{\langle \dot{X}^2|X=x'\rangle}dx'\right], \tag{5}$$

where an overdot indicates a time derivative and C_N is a constant fixed by normalization. The quantity $\langle \dot{X}^2|X=x\rangle$ denotes the average of the square of the time derivative of $X(t)$ when X is at a given value x. It is thus a conditional average and is generally a function of x. The conditional average of the second time derivative $\langle \ddot{X}|X=x\rangle$ is defined similarly. It is convenient to normalize the two conditional averages by defining two functions $q(x)$ and $r(x)$, respectively, as $q(x)\equiv\langle \dot{X}^2|X=x\rangle/\langle \dot{X}^2\rangle$ and $r(x)\equiv\langle \ddot{X}|X=x\rangle/\langle \dot{X}^2\rangle$. When the PDF is symmetric, $r(x)$ and $q(x)$ have been found to be, respectively, an odd and an even function [19]. We study the two functions $q(x)$ and $r(x)$ at different locations for both $A=0$ and $A\neq 0$. Interestingly, we find that $r(x)$ remains an odd function even when the PDF is skewed. Moreover, $r(x)$ is unaffected by the presence of the large-scale flow. Hence, the skewness of the PDF is solely related to the asymmetry

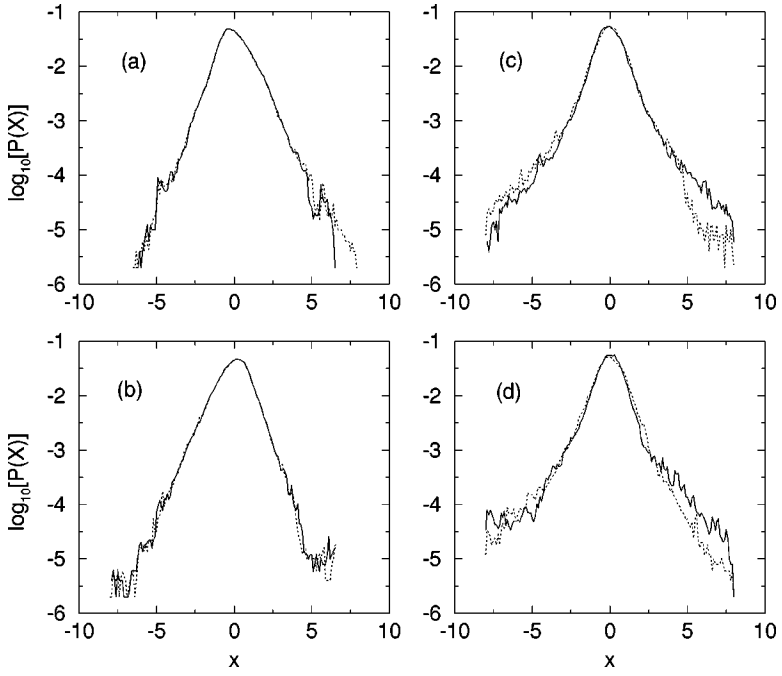

FIG. 6. Comparison of the PDFs for $A=0$ (dotted) and $A/u_0=0.05$ (solid) at various locations: (a) $(i=16,j=1)$, (b) $(i=16,j=31)$, (c) $(i=1,j=16)$, (d) $(i=31,j=16)$.

in the conditional average $q(x)$. In. Fig. 8, we plot $q(x)$ for $A\neq 0$ at various locations. Suppose $P(x>0)>P(-x)$ such that it is more probable to have positive fluctuation. Using Eq. (5) with $r(x>0)=-r(-x)$, we have $q(x>0)>q(-x)$, which implies that the typical rate of change of the scalar fluctuation is also larger for positive fluctuation. This is verified by $q(x)$ at $(i=16,j=1)$ [solid line in Fig. 8(a)]. Similar arguments hold for the case when $P(x<0)>P(-x)$.

Besides studying the one-point statistics, we have also studied the statistics of the scalar increments. We evaluate the PDFs of the scalar increments $T_\tau(i,j,t)\equiv T(i,j,t+\tau)-T(i,j,t)$, denoted by $P(T_\tau)$, for various values of τ, and also the PDFs of the scalar derivative $dT(i,j,t)/dt$ (which is just the scalar increment in the limit of $\tau\to 0$) at five locations: $a\equiv(i=2,j=16)$, $b\equiv(i=30,j=16)$, $c\equiv(i=16,j=16)$, $d\equiv(i=16,j=2)$, and $e\equiv(i=16,j=30)$. As the scalar fluctuations have time-reversal symmetry, both $P(T_\tau)$ and $P(dT/dt)$ are even functions.

In the absence of the mean flow $(A=0)$, we find that [see Fig. 9(a)] $P(T_\tau)(a)=P(T_\tau)(b)$ while $P(T_\tau)(c)\approx P(T_\tau)(d)=P(T_\tau)(e)$. The two groups of PDFs have different widths as measured by their standard deviation σ_τ:

$$\sigma_\tau(a)=\sigma_\tau(b)>\sigma_\tau(c)\approx\sigma_\tau(d)=\sigma_\tau(e) \quad \text{for } A=0. \quad (6)$$

The relative order of σ_τ follows that of σ and σ_τ's are larger when τ is larger as the average value of T_τ is larger. The same relation between the PDFs at the five different locations is found for the the PDFs of scalar derivative.

Similar observations are found when there is a large-scale flow. For a certain value τ, $P(T_\tau)(a)=P(T_\tau)(b)$ and $P(T_\tau)(d)=P(T_\tau)(e)$, and the two sets of PDFs are different from $P(T_\tau)(c)$ [see Fig. 9(b)]. The ordering of the widths of the PDFs is reversed:

$$\sigma_\tau(a)=\sigma_\tau(b)<\sigma_\tau(c)<\sigma_\tau(d)=\sigma_\tau(e) \quad \text{for } A\neq 0 \quad (7)$$

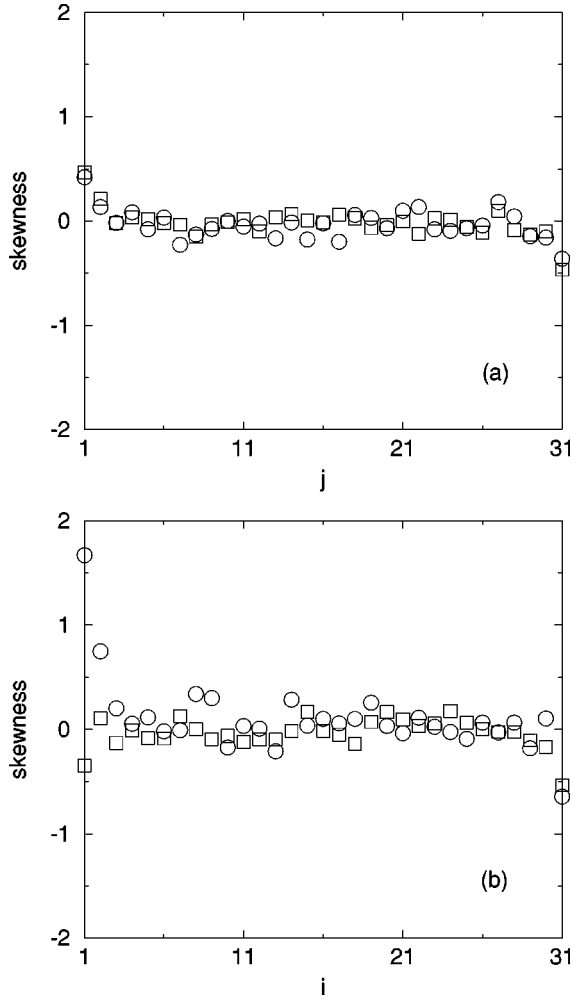

FIG. 7. Skewness of the PDF as a function of position for $A=0$ (squares) and $A/u_0=0.05$ (circles); (a) along $i=16$ and (b) along $j=16$.

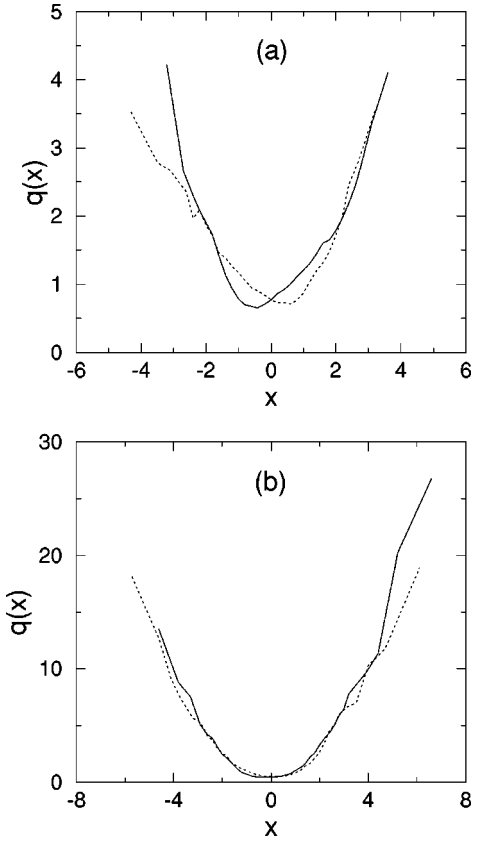

FIG. 8. Comparision of the conditional average $q(x)$ in the case with mean large-scale flow for (a) the top and bottom boundaries: $(i=16,j=1)$ (solid line) and $(i=16,j=31)$ (dotted line) and (b) the two sides: $(i=1,j=16)$ (solid line) and $(i=31,j=16)$ (dotted line).

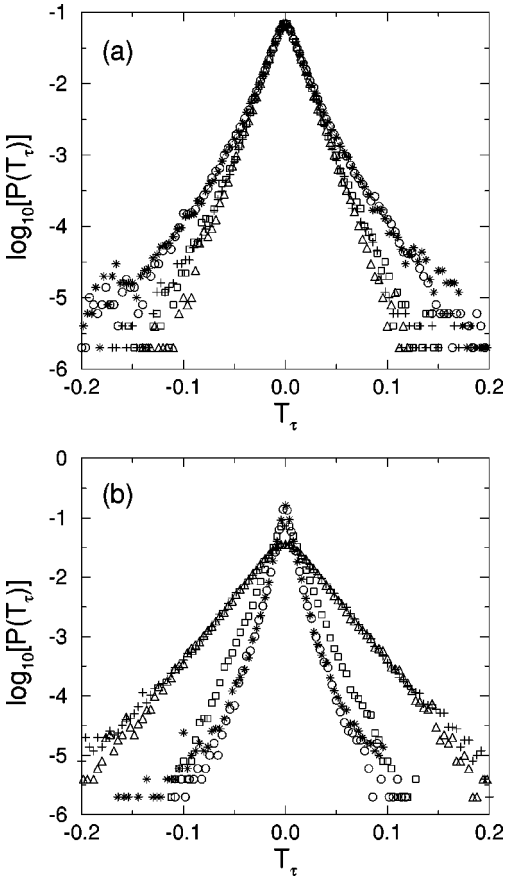

FIG. 9. The PDFs of the scalar increments T_τ, $P(T_\tau)$, for $\tau=0.6\tau_c$ at the five locations: $(i=2,j=16)$ (circles), $(i=30,j=16)$ (stars), $(i=16,j=16)$ (squares), $(i=16,j=2)$ (triangles), and $(i=16,j=30)$ (pluses) for (a) $A=0$ and (b) $A/u_0=0.05$.

following the relative order of σ.

When we normalize all the PDFs $P(T_\tau)$ and $P(dT/dt)$ by their widths, we find that the normalized PDFs $P(X_\tau)$, where $X_\tau \equiv T_\tau/\sigma_\tau$, fall into two forms no matter whether there is a mean flow or not. The first one is for locations a and b on the two sides while the other one is for locations c, d, and e on the axis. As shown in Fig. 10, the shape of the normalized PDFs on the two sides is more stretched than that for the PDFs on the axis. Hence the shape of the PDFs of the scalar increments is not affected by the presence of the large-scale flow.

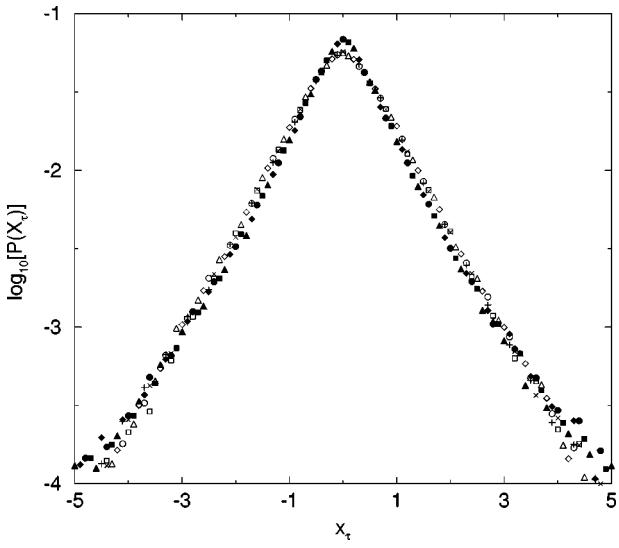

FIG. 10. Normalized PDFs of the scalar increments, $P(X_\tau)$, for $\tau=0.6\tau_c$ at the five locations for both $A=0$ and $A/u_0=0.05$. $(i=2,j=16)$: $A=0$ (filled circles); $A/u_0=0.05$ (filled rhombuses), $(i=30,j=16)$: $A=0$ (filled squares); $A/u_0=0.05$ (filled triangles), $(i=16,j=16)$: $A=0$ (crosses); $A/u_0=0.05$ (plusses), $(i=16,j=2)$: $A=0$ (circles); $A/u_0=0.05$ (rhombuses), and $(i=16,j=30)$: $A=0$ (squares); $A/u_0=0.05$ (triangles).

IV. SUMMARY

We have studied numerically the effects of a large-scale circulating flow in passive scalar advection using a two-dimensional lattice model. Various interesting features are found. First, the existence of the large-scale flow changes the mean scalar profile significantly by creating two regions of relatively larger scalar gradient near the top and the bottom boundaries and thus enhances the transfer of heat [22]. The rms scalar fluctuation profile is also altered such that two maxima are observed near the top and the bottom boundaries. The modified profiles resemble the mean and rms temperature profiles observed in turbulent convection. Thus, profiles of such shape are a direct consequence of the large-scale flow no matter whether it is generated self-consistently by the applied temperature difference as in thermal convection

or is imposed as in our model. Moreover, the magnitude of the rms fluctuation is of the order of the product of the velocity correlation length and the local mean scalar gradient, as predicted in Ref. [14], whenever the PDF is close to an exponential. In the presence of the large-scale flow, the PDFs of the scalar fluctuation near the two sides become skewed and with opposite signs. Interestingly, the conditional average $r(x)$ remains an odd function even when the PDF is skewed. Moreover, $r(x)$ is unaffected by the presence of the large-scale flow. Therefore, the skewness of the PDF is solely related to the asymmetry in the conditional average $q(x)$. Hence, whenever it is more probable to have positive fluctuations, the typical rate of change of the fluctuation is also larger for positive fluctuations. Finally, the form or shape of the PDFs of the scalar increments is found to be unaltered by the large-scale flow. This result supports the idea that large-scale effects can be filtered out by studying increments.

ACKNOWLEDGMENT

This work is supported in part by the Hong Kong Research Grant Council under Grant No. 458/95P.

[1] E. D. Siggia, Annu. Rev. Fluid Mech. **26**, 137 (1994), and references therein.
[2] F. Heslot, B. Castaing and A. Libchaber, Phys. Rev. A **36**, 5870 (1987); M. Sano, X.-Z. Wu, and A. Libchaber, *ibid.* **40**, 6421 (1989).
[3] See E. A. Spiegel, Annu. Rev. Astron. Astrophys. **9**, 323 (1971); W. V. R. Malkus, Proc. R. Soc. London, Ser. A **225**, 196 (1954); L. N. Howard, J. Fluid Mech. **17**, 405 (1963).
[4] R. Krishnamurti and L. N. Howard, Proc. Natl. Acad. Sci. USA **78**, 1981 (1981); M. Sano, X. Z. Wu, and A. Libchaber, Phys. Rev. A **40**, 6421 (1989).
[5] B. Castaing *et al.*, J. Fluid Mech. **204**, 1 (1989).
[6] B. I. Shraiman and E. D. Siggia, Phys. Rev. A **42**, 3650 (1990).
[7] A. Tilgner, A. Belmonte, and A. Libchaber, Phys. Rev. E **50**, 269 (1994).
[8] B. I. Shraiman and E. D. Siggia, Physica D **97**, 286 (1996).
[9] S. Ciliberto, S. Cioni, and C. Laroche, Phys. Rev. E **54**, R5901 (1996).
[10] E. S. C. Ching, Phys. Rev. E **55**, 1189 (1997).
[11] K. Q. Xia and S. L. Lui, Phys. Rev. Lett. **79**, 5006 (1997).
[12] Y. G. Sinai and V. Yakhot, Phys. Rev. Lett. **63**, 1962 (1989).
[13] H. Chen, S. Chen, and R. H. Kraichnan, Phys. Rev. Lett. **63**, 2657 (1989).
[14] A. Pumir, B. I. Shraiman, and E. D. Siggia, Phys. Rev. Lett. **66**, 2984 (1991).
[15] R. Bhagavatula and C. Jayaprakash, Phys. Rev. Lett. **71**, 3657 (1993).
[16] M. Holzer and A. Pumir, Phys. Rev. E **47**, 202 (1993).
[17] E. S. C. Ching and Y. Tu, Phys. Rev. E **49**, 1278 (1994).
[18] M. Chertkov, G. Falkvoich, I. Kolokolov, and V. Lebedev, Phys. Rev. E **51**, 5609 (1995).
[19] E. S. C. Ching and Y. K. Tsang, Phys. Fluids **9**, 1353 (1997).
[20] S. Cioni, S. Ciliberto, and J. Sommeria, J. Fluid Mech. **335**, 111 (1997).
[21] S. B. Pope and E. S. C. Ching, Phys. Fluids A **5**, 1529 (1993); E. S. C. Ching, Phys. Rev. E **53**, 5899 (1996).
[22] L. P. Kadanoff (private communications).